

ROTOR BROKEN BAR DIAGNOSIS IN ASD USING INSTANTANEOUS POWER SPECTRUM AND MEAN ABSOLUTE DIFFERENCE APPROACH – A COMBINED TECHNIQUE

H.H. Hanafy A. M. Hussien E. A. El-Zahab

Electrical Power and Machines Department, Faculty of Engineering, Cairo University, Giza-Egypt, Zip 12613,
e-mails: Hanafy_Hassan@hotmail.com, eng.ahmed.hussien@hotmail.com, zahab0@yahoo.com

Abstract: Rotor broken bars is a common fault in squirrel cage induction motors. Rotor failures due to that fault, now account for a moderate percentage of total induction motor failures. This paper will deal with detection of broken rotor bar of an induction motor which is supplied from adjustable speed drive (ASD) equipped with AC reactor and sine-wave shaping filter on the output side. The experimental results show that the instantaneous power spectrum (IPS) analysis method is only effective when the motor is supplied from sinusoidal supply, in contrast for the demonstrated ASD. So the instantaneous power spectrums of the healthy rotor case and the broken bar rotor cases is processed with mean absolute difference (MAD) algorithm to investigate the dissimilarity between them. The results show that this combined technique is highly effective in diagnosis of broken rotor bar fault in case of ASD.

Key words: Fault diagnosis, induction motor, rotor broken bars, instantaneous power spectrum, mean absolute difference.

1. Introduction

The Squirrel cage induction motors (SCIM) are widely used in the industrial drive fields today. In order to avoid reduced output, emergency maintenance costs, broken down equipment, and lost revenues caused by faults, it is important to detect an upcoming motor fault as soon as possible.

Generally various monitoring techniques for fault detection were used by researchers. [1-2] reviewed a large number of publications covering the different types of induction motor faults. A comparison and performance evaluation of different diagnostic procedures that use input electric signals to detect and quantify rotor breakage in SCIM supplied by the mains have been performed in [3]. Authors in [4] used the air-gap torque spectra as a potential signature for online condition monitoring and fault diagnosis in SCIM. One of the most well-known

approaches regarding the diagnosis of rotor faults in induction machines is based on online monitoring and processing of the stator currents. The main advantages and drawbacks of motor current signal processing techniques for induction motor rotor fault detection (mainly broken bars and bearing deterioration) have been presented in [5].

The Fast Fourier Transform (FFT) method is successfully used for the rotor fault detection in the SCIM. G. Didier et al. have presented a new technique to detect broken rotor bars in poly phase induction machines, by employing the Fourier Transform of the stator current to analyze its phase combined with the Hilbert Transform [6]. Toomas Vaimann et al. in [7] analyzed the diagnostic possibilities of three-phase squirrel-cage induction motor rotor faults through the implementation of FFT.

Diagnosis of mixed broken rotor bars and eccentricity faults in SCIM using instantaneous power spectrum has been investigated by Zhenxing Liu et al. in [8]. Diagnosis based on the global fault index method applied to the instantaneous power signal and line current signal provides relevant results for the detection of broken rotor bars has been presented in [9].

Recently a powerful mathematical tool known as Wavelet Transform (WT) has been used which can diagnose rotor broken bar fault. M. Riera et al. introduced a new method for the diagnosis of rotor broken bar in induction machines based on the application of the Discrete Wavelet Transform (DWT) to detect the stator current harmonic of a particular frequency variation during the startup process, when a rotor broken bar occurs [10]. The detection of rotor faults in induction machines by applying a newly developed quantification technique based on the wavelet transform to the envelope of the

starting current of the machine, has been presented in [11]. Induction motor fault diagnosis method based on three-phase stator current envelopes for broken rotor bars and inter-turn short circuits has been presented in [12]. A new Beirut diagnostic procedure (BDP) uses only two of the three motor supply currents and does not need any voltage sensors installation, has been presented by Mario Eltabach et al. in [13], as a new non-invasive electrical diagnostic method for detection of broken rotor bars in induction motors. Experimental results of sensorless broken bar detection in induction motors based on fluctuations of the stator current zero crossing instants before actual breakdown occurs have been presented in [14]. Boudinar et al. used an improved Root-MUSIC (Multiple Signal Classification) approach as powerful tool for extracting meaningful frequencies from the stator current to improve the diagnosis of rotor broken bar of the induction motor [15].

This paper presents an experimental study of instantaneous power spectrum (IPS) technique in case of sinusoidal supply and the same technique combined with mean absolute difference approach in case of special ASD for diagnosis of the broken bar fault.

Two common rotor broken bar faults are considered; one broken bar and two adjacent broken bars. In the proposed technique the instantaneous power spectrums of the healthy rotor case and the broken bar rotor cases is processed with mean absolute difference (MAD) algorithm to investigate the dissimilarity between them.

2. Instantaneous Power Signature Technique

Assuming a healthy motor with no speed oscillation, has an ideal three phase supply voltage with instantaneous phase voltage of $v_s(t)$ and an instantaneous phase current of $i_s(t)$, the instantaneous power $P_s(t)$ can be written as follows [9]:

$$v_s(t) = \sqrt{2}V_s \cos(\omega t) \quad (1)$$

$$i_s(t) = \sqrt{2}I_s \cos(\omega t - \varphi) \quad (2)$$

$$P_s(t) = V_s I_s [\cos(2\omega t - \varphi) + \cos(\varphi)] \quad (3)$$

Where φ = the motor phase angle.

As shown from (2) and (3), the current spectrum has only one component at a frequency of f_s ($f_s = \omega/2\pi$), while the power spectrum has two components, DC component and the other component at a frequency of f_c ($f_c = \omega/\pi$).

When broken bars fault occurs, a rotor asymmetry takes place, causing the appearance of additional

two frequency components, the lower component is due to backward rotating field resulting from the broken bar fault and the upper component is due to torque pulsation and speed oscillation. These components occur at frequencies given by [2], [9]:

$$f_{bb} = (1 \pm 2KS) f_s \quad (4)$$

Where:

$$K = 1, 2, 3 \dots$$

S = operating per unit slip of the motor.

The lower frequency component magnitude is not equal to the upper frequency component [8-9]. So in case of broken bars, the mathematical expression of the instantaneous power of a squirrel cage induction motor is given by [9]:

$$P_s(t) = V_s I_s [\cos(2\omega t - \phi) + \cos\phi] +$$

$$\sum_{K=1}^{\infty} V_s I_{b_{pk}} [\cos(2(1-ks)\omega t - \phi_{b_{pk}}) + \cos(2ks\omega t + \phi_{b_{pk}})] + (5)$$

$$\sum_{K=1}^{\infty} V_s I_{b_{nk}} [\cos(2(1+ks)\omega t - \phi_{b_{nk}}) + \cos(2ks\omega t - \phi_{b_{nk}})]$$

Where:

$I_{b_{pk}}$: RMS value of the current spectrum component at frequency $(1-2kS)f_s$

$I_{b_{nk}}$: RMS value of the current spectrum component at frequency $(1+2kS)f_s$

$\phi_{b_{pk}}$: Initial phase angle of the current spectrum component at the frequency $(1-2kS)f_s$

$\phi_{b_{nk}}$: Initial phase angle of the current spectrum component at the frequency $(1+2kS)f_s$

3. Mean Absolute Difference Approach

The Mean Absolute Difference (MAD) is a widely used in signal processing applications to investigate the dissimilarity between two vectors [16]. It is often used for real-time implementation, because it is computationally very efficient.

In our proposed technique, the MAD is used to investigate the dissimilarity between two vectors, these vectors are the instantaneous power spectrum of the predetermined reference vector (healthy cage) and the examined vectors (broken bars cages) at different operating speeds of the ASD. The MAD is given by [16]:

$$MAD = \frac{1}{n} \sum_{m=0}^{n-1} |A_m - B_m| \quad (6)$$

Where:

n: Length of the vectors

A_m : Reference vector (Healthy case)

B_m : Examined vector for each case

4. Experimental Results and Discussion

The motor under test has been chosen as 3 HP, 2-pole, 380 V and 50 Hz cage induction motor drives a water pump. The test bed block diagram is shown in Fig.1, which consists of current and voltage transducers from LEM and their part numbers are LTS 25-NP, LV 100-400 respectively and the data acquisition system is NI PCI-6251 16-Bit, 1 MS/s with connection board connected to the IBM compatible PC, the diagnosis software is implemented on NI LabView; the results documentation and formatting by using NI Diadem.

The stator voltages and currents were sampled at 20 KHz individually for 10 seconds of steady state operation, which gives a 0.1 Hz spectrum resolution with 10 KHz full scale spectrum. Voltage and current waveforms are multiplied together to get the instantaneous power waveform and fast Fourier transform is applied. The experimental data limited to frequency components $(2 \pm 2KS)f_s$, with $K=1, 2$. The discussions will be demonstrated in the following sections:

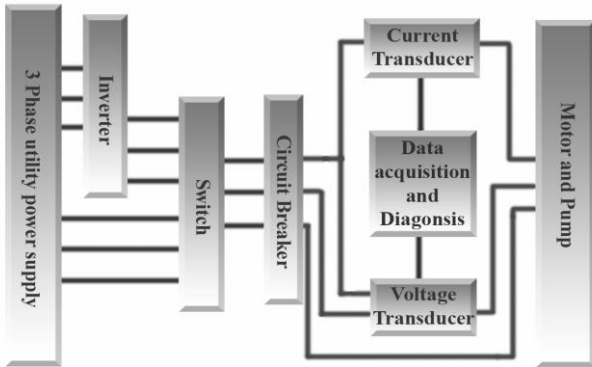


Fig.1 The test bed block diagram

4.1. Instantaneous Power spectrum of healthy and broken bars cages in case of sinusoidal supply

Fig.2 shows the instantaneous power spectrum of the healthy cage with existing lower and upper sideband frequency components, these components exist even in the healthy case due to magnetic and electrical asymmetries from the manufacturing process. Figs.3-4 show the instantaneous power spectrum of the broken bar cage cases. According to the results, a moving average scheme is applied which will be the reference instead of the zero point. Table (1) shows the amplitude of the sideband components referenced from the calculated average and the speed of each case.

From Table 1 and Figs. 2-4, the broken bar fault can be easily detected by noticing the amplitude of

the sideband components (for different fault cases there is boosting in the sidebands amplitude), which shows that the IPS method is highly effective in diagnosis of the broken bar fault under different fault cases when the supply voltage is sinusoidal.

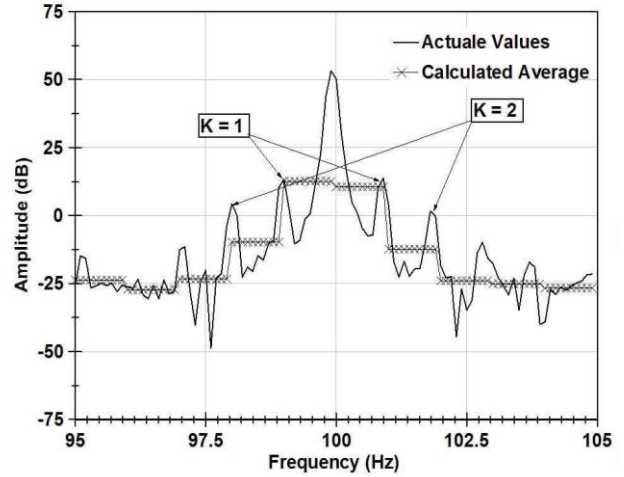


Fig. 2 The IPS of healthy cage for sinusoidal supply

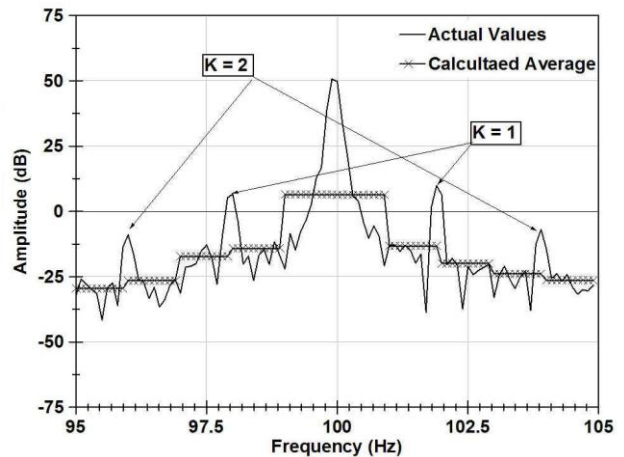


Fig. 3 The IPS of one broken bar cage for sinusoidal supply

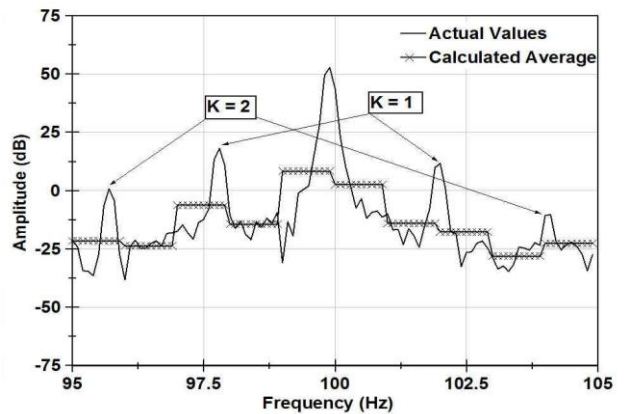


Fig. 4 The IPS of two adjacent broken bars cage for sinusoidal supply

Table 1 The amplitude of the sideband components referenced from the calculated average and the speed of each case.

Motor Status	K=1	K=1	K=2	K=2	Speed (rpm)
	left (dB)	right (dB)	left (dB)	right (dB)	
Healthy	0.62	3.24	14.07	13.93	2970
One Broken Bar	20.74	23.08	17.58	16.94	2943
Two Adj. Broken Bars	24.41	29.44	22.29	17.8	2930

4.2. Instantaneous Power Spectrum of Healthy and Broken Bars Cages in Case of ASD

The waveform of the inverter output voltage at 50 Hz is shown in Fig.5; mainly the difference in the waveform from the traditional inverter is due to the built in output side AC reactor and Sin-wave shaping filter. The main function of the filter and the reactor is to reduce the vibration in the motor caused by inverter switching waveforms. This is the case of high power motor in range of 200 HP inverters, where the vibration consideration is important.

The results shown in this section are the instantaneous power spectrums at the supply frequencies of 45 Hz in Figs.6-8, 50 Hz in Figs.9-11 and 55 Hz in Figs. 12-14.

By noticing Figs. 6-14, one can conclude that, there are no identification sideband frequencies as in case of the sinusoidal supply. According to these results, the instantaneous power spectrum method is not effective in the case of special inverter case (ASD), in contrast with the sinusoidal supply case.

4.3. The Proposed Combined Technique

In [16], the MAD was applied as follows; extract appropriate features that contain useful fault signature (upper and lower sideband) in the spectral information while suppressing other spectral information such as fundamental and noise components. After the appropriate features are extracted, the reference (healthy) and examined (broken bar) vectors are compared using (6) for detection of the broken bar fault.

In the proposed technique, The MAD was calculated as follows; the healthy, one broken bar and two adjacent broken bars cages instantaneous power was acquired using the proposed test-bed the reference vector will be the instantaneous power spectrum of the healthy case, and the examined vector will be the instantaneous power spectrum of the fault case at the same supply frequency and load

conditions, without removing any components from the spectrum.

The MAD is used to search for hidden information in the spectrum. Table 2 shows MAD magnitude versus supply frequency at different fault cases. Fig.15 shows the calculated MAD for one broken bar and two adjacent broken bars cages versus the supply frequency. It is clearly that combined technique is highly effective in diagnosis of broken rotor bar fault in case of ASD.

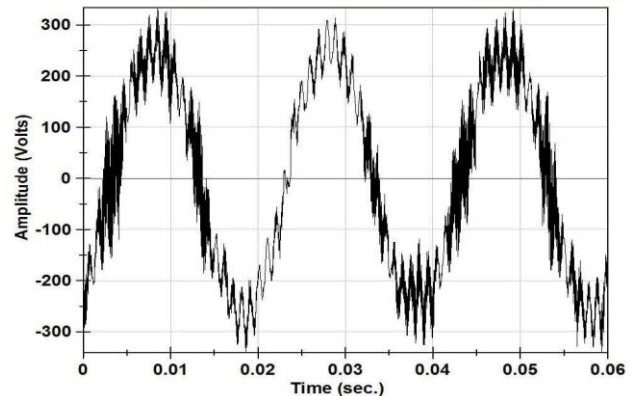


Fig.5 Waveform of the inverter output voltage at 50 Hz

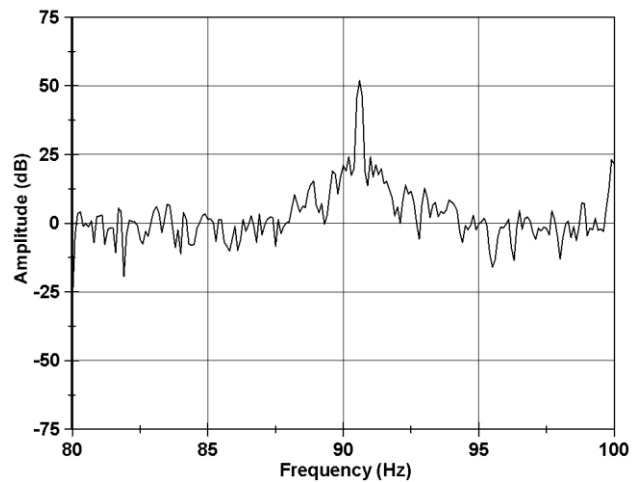


Fig.6 The IPS of the healthy cage supplied from inverter at 45 Hz

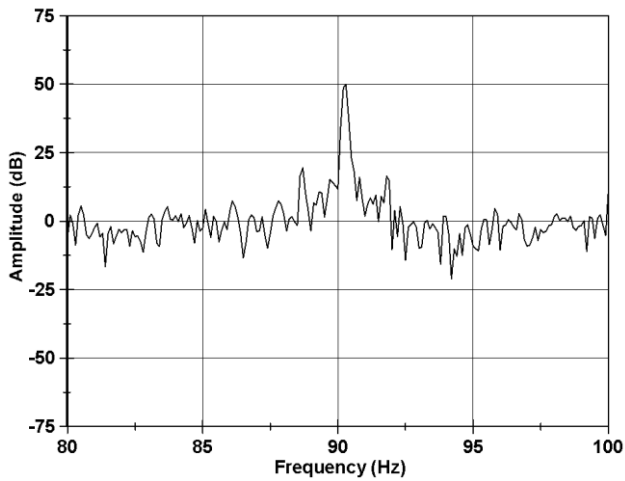


Fig.7 The IPS of one broken bar cage supplied from inverter at 45 Hz

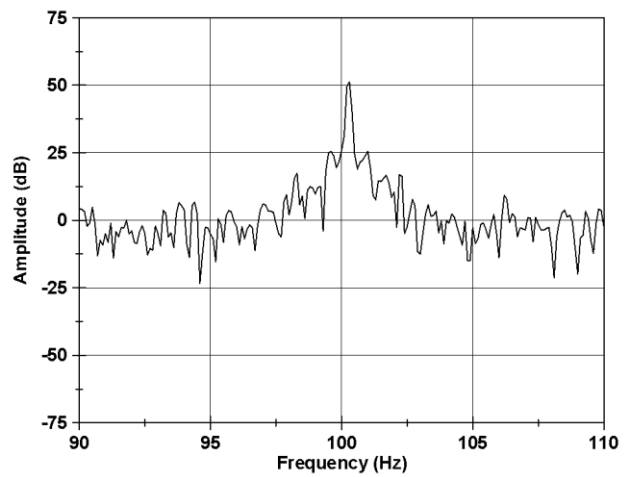


Fig.10 The IPS of one broken bar cage supplied from inverter at 50 Hz

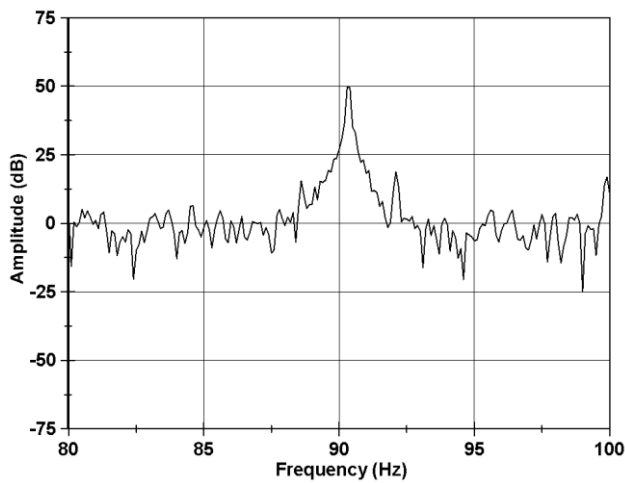


Fig.8 The IPS of two adjacent broken bars cage supplied from inverter at 45 Hz

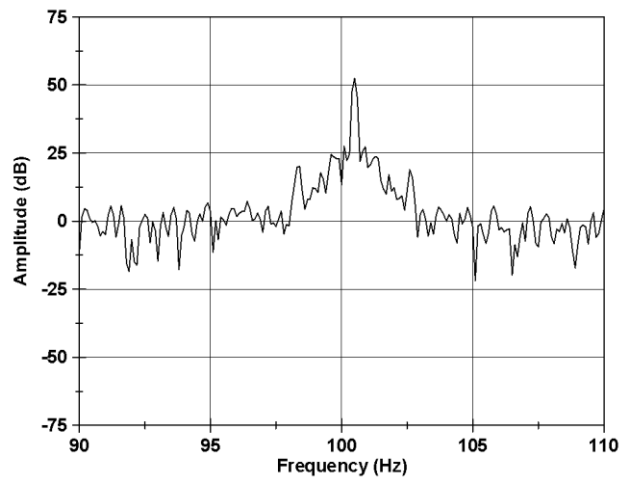


Fig.11 The IPS of two adjacent broken bars cage supplied from inverter at 50 Hz

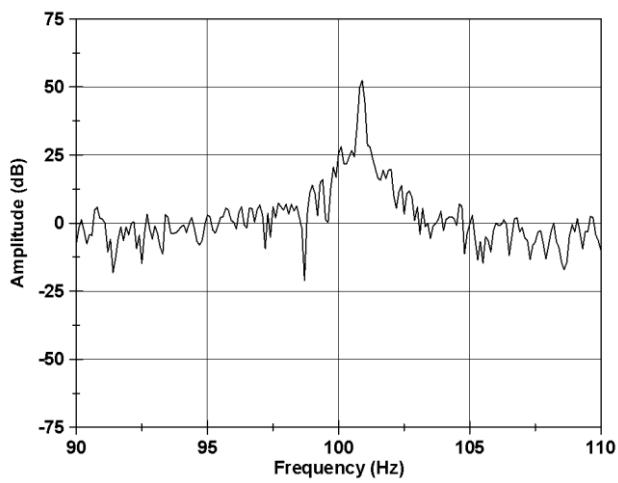


Fig.9 The IPS of the healthy cage supplied from inverter at 50 Hz

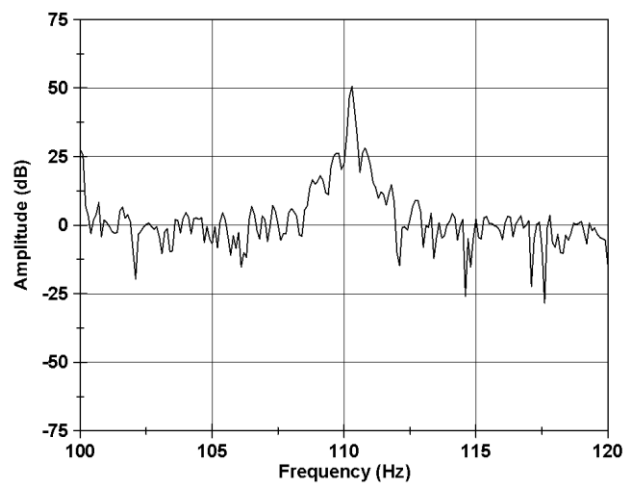


Fig.12 The IPS of the healthy cage supplied from inverter at 55 Hz

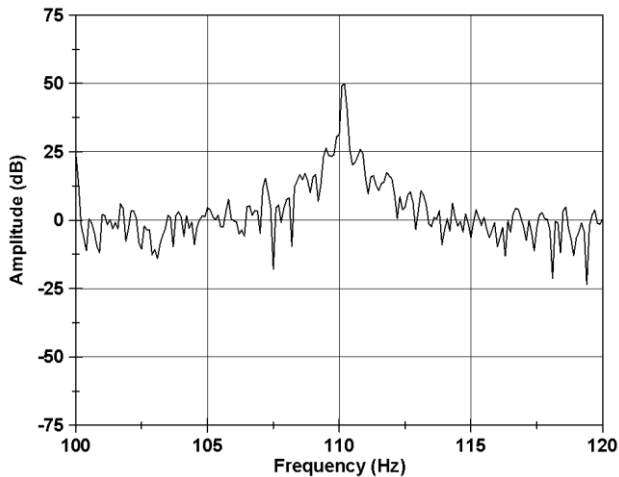


Fig.13 The IPS of one broken bar cage supplied from inverter at 55 Hz

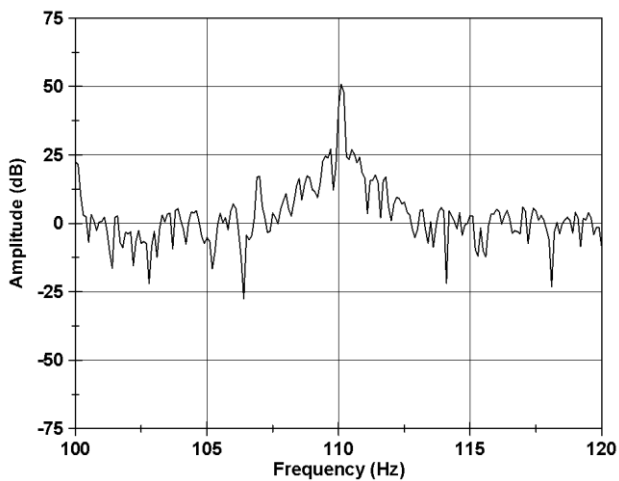


Fig.14 The IPS of two adjacent broken bars cage supplied from inverter at 55 Hz

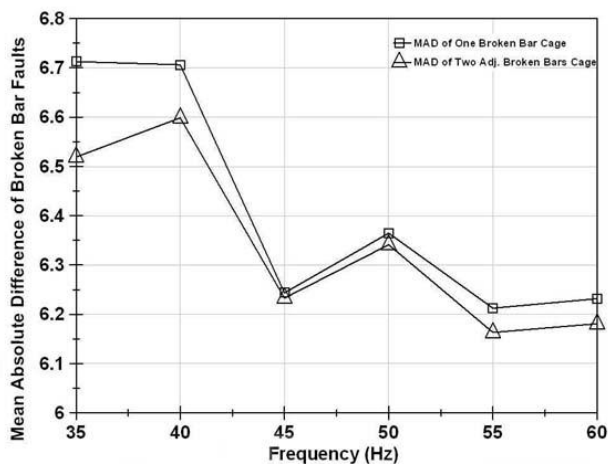


Fig.15 MAD magnitude versus supply frequency at different fault cases

5. Conclusion

In this paper, the Instantaneous Power Spectrum technique in the diagnosis of induction motor broken bar fault is investigated through sinusoidal and special inverter source (ASD), this investigation shows the performance of this technique in both cases. It is found that, this technique is effective on the diagnostics for the sinusoidal supply case, in contrast for the special inverter case. This result, leads on using one of popular digital processing technique, which is the Mean Absolute Difference approach (MAD) to compare different instantaneous power spectrums at fault cases with the healthy instantaneous power spectrum at the same operating conditions to search for hidden information in the faulty spectrums. The results were satisfactory, and show the potential of the proposed technique. The combined technique is very computationally efficient, and with the digital technology available now, an embedded system could be designed for that purpose with economical price.

References

1. Arfat Siddique, Yadava G. S. and Bhim Singh: *A Review of Stator Fault Monitoring Techniques of Induction Motors*. In: IEEE Trans. on Energy Conversion, vol. 20, no. 1, March 2005, p. 106 - 114,.
2. Subhasis Nandi, Hamid A. Toliyat and Xiaodong Li: *Condition Monitoring and Fault Diagnosis of Electrical Motors—A Review*. In: IEEE Trans. on Energy Conversion, vol. 20, no. 4, December 2005, p. 719-729.
3. Bellini A., Filippetti F. , Franceschini G., Tassoni C. and Kliman G.B.: *Quantitative Evaluation of Induction Motor Broken Bars By Means of Electrical Signature Analysis*. In: Industry Applications Conference, 2000. Conference Record of the 2000 IEEE, Issue, 2000, vol.1, p. 484 – 491.
4. Vinod V. Thomas, Krishna Vasudevan and Jagadeesh Kumar V.: *Online Cage Rotor Fault Detection Using Air-Gap Torque Spectra*. In: IEEE Trans. on Energy Conversion, vol. 18, no. 2, June 2003, p. 265 - 270.
5. Mohamed El Hachemi Benbouzid, and Gerald B. Kliman: *What Stator Current Processing-Based Technique to Use for Induction Motor Rotor Faults Diagnosis?* In: IEEE Trans. on Energy Conversion, vol. 18, no. 2, June 2003, p. 238 – 244.
6. Didier G., Ternisien E., Caspary O. and Razik H.: *A new approach to detect broken rotor bars in induction machines by current spectrum analysis*. In: Elsevier, Mechanical Systems and Signal Processing, vol. 21, 2007, p. 1127–1142.
7. Toomas Vaimann and Ants Kallaste: *Detection of broken rotor bars in three-phase squirrel-cage induction motor using fast Fourier transform*. In: 10th International Symposium on Topical Problems in the Field of Electrical

and Power Engineering, Pärnu, Estonia, January 10-15, 2011, p. 52-56.

8. Zhenxing Liu, Xianggen Yin, Zhe Zhang, Deshu Chen and Wei Chen: *Online Rotor Mixed Fault Diagnosis Way Based on Spectrum Analysis of Instantaneous Power in Squirrel Cage Induction Motors*. In: IEEE Trans. on Energy Conversion, vol. 19, no. 3, September 2004, p. 485 – 490.

9. Gaëtan Didier, Eric Ternisien, Olivier Caspary, and Hubert Razik: *Fault Detection of Broken Rotor Bars in Induction Motor Using a Global Fault Index*. In: IEEE Trans. on Industry Applications, vol. 42, no. 1, January/February 2006, p. 79 - 88.

10. Riera M., Antonino J.A., Roger-Folch J., and Molina M.P.: *Detection of Broken Rotor Bars in Induction Machines through the Study of the Startup Transient via Wavelet Decomposition*. In: Journal of Electrical Engineering (JEE), Vol.6, No.3, 2006, p.18-25.

11. Khadim Moin Siddiqui and Giri V.K.: *Broken Rotor Bar Fault Detection in Induction Motors using Transient Current Analysis*. In: International Journal of electronics & communication technology (IJECT), vol. 2, no. 4, Dec. 2011, p. 114-119.

12. Aderiano M. da Silva, Richard J. Povinelli, and Nabeel A. O. Demerdash: *Induction Machine Broken Bar and*

Stator Short-Circuit Fault Diagnostics Based on Three-Phase Stator Current Envelopes. In: IEEE Trans. on Industrial Electronics, vol. 55, no. 3, 2008, p. 1310 - 1318.

13. Mario Eltabach, Jerome Antoni, Galyna Shanina, Sophie Sieg-Zieba and Xavier Carniel: *Broken rotor bars detection by a new non-invasive diagnostic procedure*. In: Elsevier, Mechanical Systems and Signal Processing, vol. 23, 2009, p.1398–1412.

14. Hakan Calis and Abdulkadir Cakir: *Experimental study for sensorless broken bar detection in induction motors*. In: Elsevier, Energy Conversion and Management vol. 49, 2008, p. 854–862.

15. Boudinar A .H., Bendiabdellah A., Benouzza N. and Boughanmi N.: *Three Phase Induction Motor Incipient Rotor's Faults Detection Based On Improved Root-Music Approach*. In: Journal of Electrical Engineering (JEE), Vol.7, No.7, 2007, p.100-107.

16. Song M. H., Kang E. S., Jeong C. H., Chow M.Y. and Ayhan B.: *Mean Absolute Difference Approach for Induction Motor Broken Rotor Bar Fault Detection*. In: SDEMPED 2003, Symposium on Diagnostics for Electric Machines, Power Electronics and Drives, Atlanta. CA, USA, 24-26 August 2003, p. 115 – 118.

Table 2 MAD magnitudes versus supply frequency.

Supply Frequency (Hz)	MAD of One Broken Bar (dB)	MAD of Two Broken Bars (dB)
35	6.71275	6.51923
40	6.70603	6.59853
45	6.24357	6.23279
50	6.36456	6.34109
55	6.21245	6.1631
60	6.23155	6.18082